Journal of Statistical Physics, Vol. 70, Nos. 1/2, 1993

Models of the Temporal Dynamics of Visual Processing

Ralph M. Siegel[1] **and Heather L. Read**[1]

Single unit recordings of neurons in primary visual cortex have demonstrated complex temporal patterns in the interspike interval return maps when presented with periodic input. Two models are tested to account for these patterns. An integrate-and-fire model is only able to replicate the *in vivo* data if its synaptic input is a chaotic function of time (such as a time series derived from the sinusoidally driven Duffing equation). Simpler purely periodic inputs are insufficient to replicate the experimental data. A Hodgkin–Huxley ionic model with a periodic input can replicate some of the features of the neural data, however it seems to be lacking as a complete model. These results indicate that the *in vivo* dynamics are not a result of the intrinsic properties of the neuron, but arise from a chaotic input to the neuron.

KEY WORDS: Cortex; vision; chaos theory; return maps; Poincaré sections; integrate-and-fire; ionic model; Duffing equation.

1. INTRODUCTION

Our understanding of visual information processing in the brain has been derived, to a large extent, from the study of single neuron activity patterns elicited with visual stimuli. By systematically altering the visual stimulus parameters (such as color, brightness, shape, and orientation), one can identify the features of a visual stimulus that elicit changes in the single neuron activity. Furthermore, one can explore the cortical distribution of neurons that respond to a common stimulus feature and begin to understand how visual stimuli are represented throughout a given population of visual sensory neurons. The measures of neural activity explored to date are primarily statistical (e.g., changes in the mean firing rate, autocorrelograms), although there have been some notable excep-

[1] Center for Molecular and Behavioral Neuroscience, Rutgers, The State University, Newark, New Jersey 07102.

0022-4715/93/0100-0297$07.00/0

tions.[1, 4, 13] Even though the standard approaches have been fruitful measures of stimulus-dependent changes in neural output, they tend to obscure some of the finer temporal patterns seen in the data. For instance, a cell that fires a single spike every 20 msec will have the same mean firing rate (50 Hz) as a cell that fires a pair of spikes every 40 msec. Clearly, the postsynaptic outcome of these two patterns would be very different. Hence, the need arises to explore the finer details of stimulus-induced temporal activity patterns.

Temporal patterns of neuronal activity such as those described above are derived from extracellular records of action potentials prior to propagation from the hilar region to the terminal region where they elicit transmitter release. The depolarizing peak of the action potential is larger than that of other ongoing extracellular events and can be reliably monitored with extracellular recording electrodes. However, the subthreshold fluctuations in membrane potential preceding the onset of an action potential are not reliably measured with extracellular recording. The latter is of no consequence to the measure of mean firing rates or other statistical measures; however, it is a confounding problem when attempting to reconstruct the underlying dynamics of the system from the data using nonlinear dynamical theory.

Reconstruction of the underlying dynamics typically proceeds by sampling a subset of the data at fixed intervals in time and is justified by the application of Takens' theorem.[19] Takens' theorem, paraphrased, states that the topological representation of the system can be equivalently reconstructed using one variable of the system with varied sampling intervals, e.g., $(X_1(t), X_1(t+\tau), X_1(t+2\tau),..., X_1(t+n\tau))$ or using the n variables of the system, e.g., $(X_1(t), X_2(t), X_3(t),..., X_n(t))$. In essence, the motion of a single variable of a complex system reflects the dynamics of the entire system. This subset of the data, when graphically depicted, is called a Poincaré section. This theorem is not directly applicable to extracellular records of interspike intervals, which are values that occur at nonfixed intervals in time. Thus, it is not immediately obvious how to form the Poincaré section and to reconstruct the underlying dynamics for neural data. As an alternative, temporal patterns of neuronal activity can be depicted with an interspike interval return map, a cousin to the Poincaré section.[18] Two-dimensional interval return maps of such data (Fig. 1) are constructed by plotting the ith interval versus the $(i+n)$th interval, with n small and typically 1.[4, 17, 18] Higher-dimensional plots to reveal higher-order effects can also be made by plotting $I_i, I_{i+1}, I_{i+2},..., I_{i+n}$, but their discussion is beyond the scope of the present study. Although such graphs do not follow the exact formalism of Takens' theorem, they follow the spirit in reaching toward a graphical representation of the temporal dynamics.

The salient features of the visual cortical neuron return maps generated

with repetitive presentations of a bar of light at a fixed period (Fig. 1) include: (1) an extended range of interspike intervals at rational multiples of the driving period, (2) asymmetries about the line $I_i = I_{i+1}$, and (3) repeated, perhaps fractal, structures at different orders of magnitude (rarely found). Furthermore, if the visual stimulus period is systematically varied, the interspike intervals undergo period-adding bifurcations. These results have been used to support the idea that the single neuron operates as an element of an interactive deterministic population.[18] If this supposition is correct, then the range of activity of the neuron should be constrained by the theory of dynamical systems. The remainder of this paper considers the structure and nature of the return map generated from

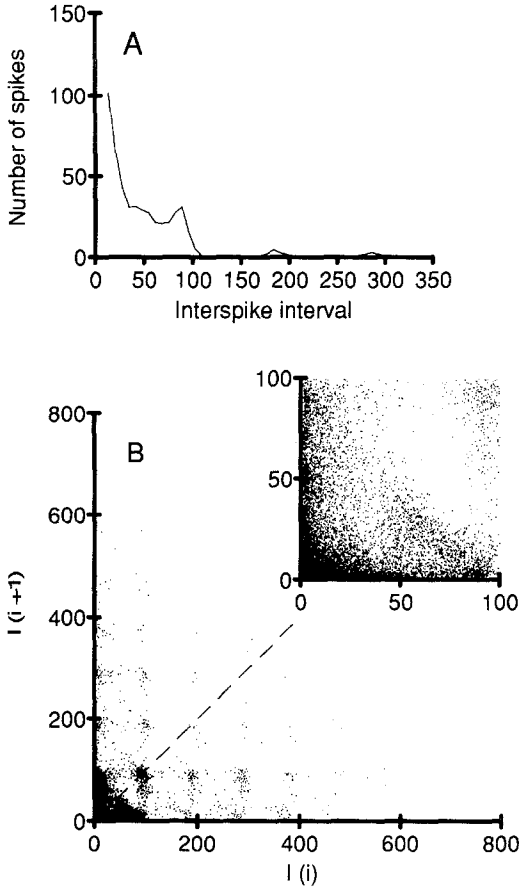

Fig. 1. Data from cat primary visual cortex. Methods were as in Siegel.[18] The interspike intervals are shown as (A) an interspike interval histogram and (B) a return map. The inset of (B) shows the fine structure of the return map. Note the extended interspike intervals and the asymmetries about the line $I_{i+1} = I_i$.

two model systems and compares and contrasts them to those derived from recordings of visual cortical neurons.

2. RESULTS

2.1. Integrate-and-Fire Models

Periodic sensory input results in complex temporal patterns of action potentials in cat visual cortex,[18] somatosensory cortex,[11] and the auditory nerve.[16] Gerstein and Mandelbrot[3] have modeled the activation of a neuron by synaptic input as a random walk of the membrane potential to a threshold. At the threshold, the action potential occurs. This model is given as

$$V_m(t+\delta t) = V_m(t) + \eta(t) + \alpha(t)\,\delta t \tag{1}$$

where $V_m(t)$ is the membrane potential of a cell, $\alpha(t)$ is the sum of excitatory and inhibitory synaptic inputs, $\eta(t)$ is uniformly distributed noise on the range $\pm N$, and δt is the time step. This equation is also called an integrate-and-fire model and has been studied in the absence of noise and with noise.[5, 9, 10] The equation is iterated until $V_m(t)$ is greater than some threshold value V_T, at which time t^* an action potential event is deemed to occur, and $V_m(t^*) = 0$.

If $\alpha(t)$ is a constant A and $\eta(t) = 0$, then the interspike intervals $I_i = t^*_{i+1} - t^*_i$ converge to a constant value of V_T/A. The return map of this would be a single point, as would the Poincaré section of the value $V_m(T^*)$. If the random walk term is a small value, then the I_i are Poisson distributed (Fig. 2B), as shown by Gerstein and Mandelbrot.[3] A return map of the interspike intervals reveals an unstructured distribution of points (Fig. 2B).

If the synaptic input is a sine wave, $\alpha(t) = A\sin(\omega t)$, the firing pattern reaches a steady state,[9] so that spiking occurs at regular intervals in phase with the driving period. In the density histogram (Fig. 2C) and the return map (Fig. 2D, arrow), these steady states are reflected by a high density of points at integer multiples of the stimulus period. The return map becomes much more interesting in the presence of the random walk; the interspike interval pairs distribute more diffusely and new interspike interval pairs appear. When $\eta(t) = 0.5$ with the same sinusoidal driving force, interspike intervals are distributed across a broader range, as illustrated in the multiple point clusters of the return map (Fig. 2F) and the multiple peaks in the density histograms (Fig. 2E). The extended range of interspike intervals and the geometric decay of peaks in the density histogram are both observed in periodically driven cortical neurons (Fig. 1). Note that the model return map (Fig. 2F) is not absolutely symmetric about the $I_i = I_{i+1}$ axis. There are complementary point clusters on either side of the dashed

line; however, within each cluster there is some asymmetry. Thus, adding a random walk can introduce (or reveal) asymmetries in interspike interval distributions or point clusters observed in return maps of the periodically driven integrate-and-fire model. These results suggest that a significant portion of the temporal patterns recorded *in situ* are explicable in terms of a simple spiking mechanism with periodic input and noise.

We next consider the return maps obtained with a chaotic modulation of the function $\alpha(t)$. The use of the chaotic function is motivated by experimental findings in which phase plots of the instantaneous firing rate

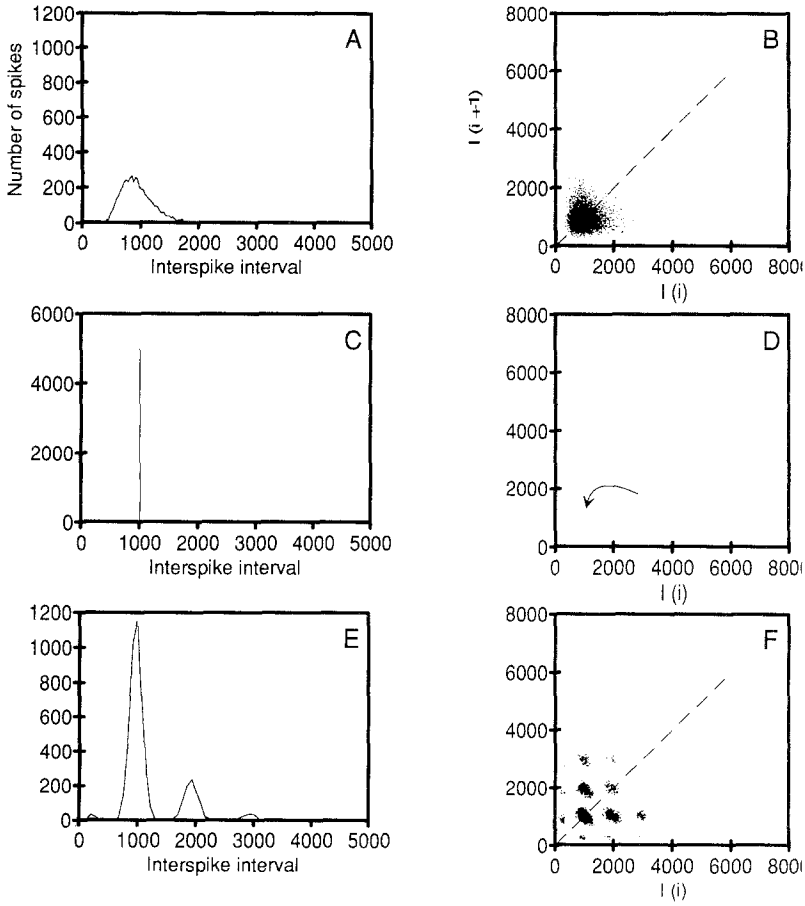

Fig. 2. Integrate-and-fire model. (A, C, E) The interspike interval density histograms and (B, D, F) return maps for the integrate-and-fire model with (A, B) a random walk to threshold [$\eta(t) = 0.01$], (C, D) sinusoidal driving force and no random walk [$\eta(t) = 0$], and (E, F) sinusoidal driving force and a random walk [$\eta(t) = 0.01$]. In (C–F) the sinusoid amplitude and period were 0.5 and 2000, respectively.

of visual neurons have a similarity to the phase plots obtained from the Duffing or Lorentz equation (Siegel, unpublished data). The chaotic attractor is given by the Duffing equation $y'' + cy' + y^3 = b\cos(t)$, with $b = 12$ and $c = 0.1$. In general the Poincaré section of the Duffing equation is taken by plotting y against y' at time $t = 2n\pi$, $n = 1, 2, \ldots$, or $y(t)$ versus $y(t + \Delta t)$.[2] This typical Poincaré section is characterized as a strange attractor with a repeating or fractal structure at multiple levels of magnitude.

By setting the stimulus input equal to one variable from the Duffing equation [e.g., $\alpha(t) = y(t)$] and iterating Eq. (1), continuous values from the Duffing equation are transformed into interspike intervals. The return maps generated with the Duffing driven "integrate-and-fire model" are not at all similar in shape to the original Poincaré section. The highly folded continuous Poincaré section of the original function is fragmented into a highly complex return map (Fig. 3B). The return map is still fractal, but the relatively simple structure of the original strange attractor is exploded into many smaller pieces. The presence of a random walk $\eta(t) \neq 0$ blurs the fine fractal structure (Fig. 3B and 3D).

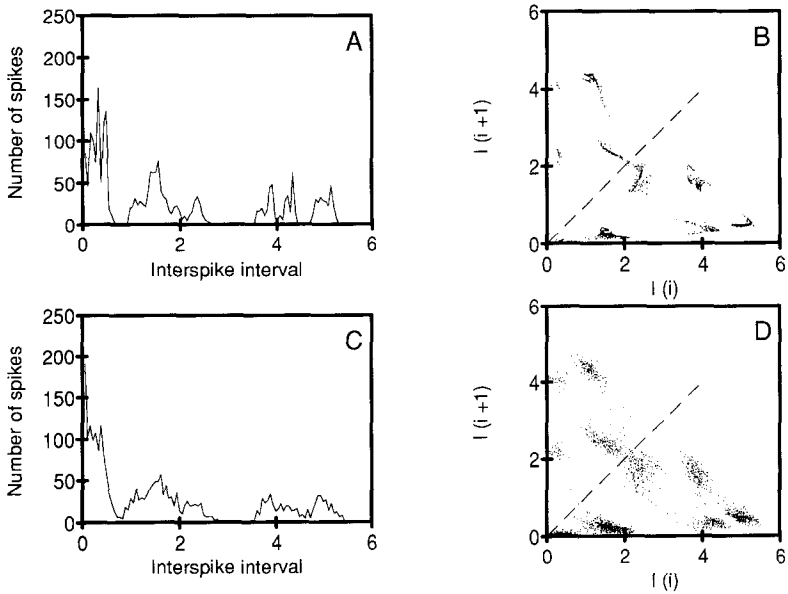

Fig. 3. Duffing driven integrate-and-fire model with and without a random walk to threshold. (A, B) Marked asymmetries in the interspike interval distribution were reflected in (A) the density histogram and (B) the return map. Not the asymmetry about $I_{i+1} = I_i$ and the focal asymmetries in the clusters of interspike interval pairs. (C, D) The focal asymmetries were less apparent when a random walk to threshold was utilized.

A striking feature of the return map generated with a Duffing driven integrate-and-fire model is the asymmetry about the $I_i = I_{i+1}$ line. Note in Figs. 3B and 3D that the point clusters are not simply mirror images of their neighbors on either side of the $I_i = I_{i+1}$ line. Furthermore, there are local asymmetries in the distribution of points within a given cluster of the return map or peak of the density histogram (Figs. 3A and 3B). Local asymmetries (possibly attractors) such these have not been described and heretofore have not been noted in the literature. Finally, the dimension of the spiking Duffing system is apparently greater than 2 because the return map has segments that cross each other. In contrast, the dimension of the original Duffing equation is an irrational number less than 2. The apparent increase in dimension with the spiking system is important to note, as prior studies have attempted to compute the dimension of the underlying dynamics with interspike interval data.[15] The current results suggest that such computations may be artificially inflated or erroneous, in agreement with Preissl *et al.*,[14] and caution against the use of quantities such as dimension to solely define the characteristics of a dynamical neural system.

These results taken together suggest that the return maps resulting from periodic flash-evoked activity in sensory cortical neurons may reflect a quasiperiodic but ordered synaptic input. Recall that $\alpha(t)$ represents the sum synaptic input to the model neuron. The input to the single neuron may indeed be chaotic, but the input need not be so formally constrained. For instance, complex patterns in cortical sensory neurons may result from intrinsic properties of the network in which it participates. Thus we see that with a relatively simple driving force (e.g., sine wave), the return map of the model output is similar to the Poincaré section of the driving function, while with more complex input there is a divergence between the shape of the two.

2.2. Single-Neuron Simulation

One might argue that the integrate-and-fire model is not a reasonable encapsulation of the single neuron, which has multiple ionic conductances that are nonlinear functions of time and voltage. We therefore have begun an investigation into the effect of periodic input upon the patterns of activity of a single neuron modeled using a set of coupled nonlinear differential equations. The Hodgkin–Huxley (HH)[7] equations that model the squid giant axon have been studied in detail and are accepted as the base representation of the ionic currents of neurons and are used as the starting point of this investigation.

A number of dynamical studies examining the behavior of the sinusoidally driven HH equations have found that the sinusoidal rhythm tends to entrain the sodium spikes so that they occur at a fixed phase of

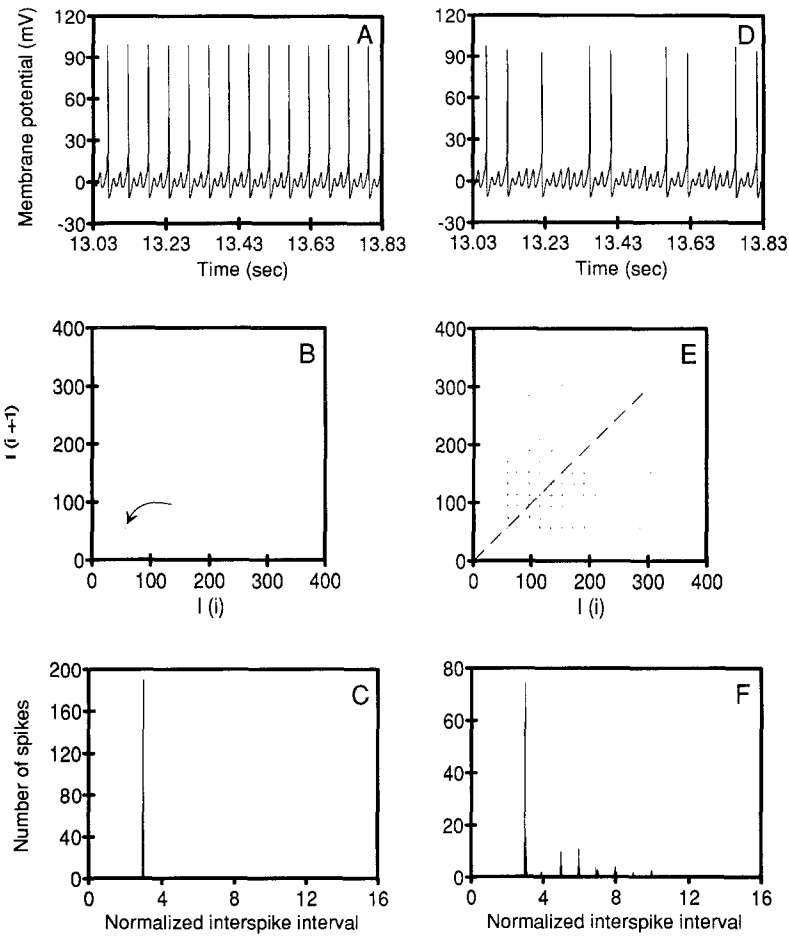

Fig. 4. Phase-locked and quasiperiodic activity with the sinusoidally driven Hodgkin–Huxley equations. (A, D) Membrane potentials, (B, E) return maps, and (C, F) interspike interval density histograms for two different cosine driving periods at an amplitude of 1.5 μA/cm^3. The driving period for (A–C) is 18.47 msec and that for (D–F) is 19.03 msec. (A) With a driving period of 18.47 msec, action potentials occur in phase (phase-locked) with the driving stimulus, generating a repetitive 3:1 (stimulus cycle:action potential) spiking pattern. B) During phase-locked activity, interspike intervals vary little, generating a return map with a single cluster of values around the point 56, 56; and (C) a high density of interspike intervals at three times the driving period. (D) When the driving period was 19.03, the pattern of action potentials was quasiperiodic or unstable. (E) During quasiperiodic activity, the range of interspike intervals was extended from a single multiple of the driving period (3) to include several integer multiples of the driving period (3, 4, 5, 6,..., 16). The extended range is reflected in both (E) the return map and (F) the density histogram. In addition, interspike interval pairs for the return map were unevenly distributed about the line $I_{i+1} = I_i$. Both simulations were run for 50 sec. The same 12 sec of each simulation is shown.

the stimulus period.[6, 8, 12] Such phase locking to the stimulus period is observed in the present study (Fig. 4A) for most of the amplitudes and frequencies explored. Consequently, the interspike intervals observed in a 50-sec simulation were clustered about a single value which was some multiple of the stimulus period (Figs. 4B and 4C). Such singular or simple interspike interval patterns are not observed *in situ* with periodic forcing.

Complex or irregular temporal spiking sequences are observed between phase-locking regions of the frequency–amplitude parameter space (Fig. 4D).[8, 12] During the course of such complex temporal patterns, interspike intervals are no longer clustered about a single value, but are distributed across several values all of which are exact or near integer multiples of the stimulus period (Figs. 4E and 4F). The extended distribution of interspike intervals observed in these unstable regions more closely resembles that of sensory neurons driven *in situ*. Furthermore, there are some asymmetries in the point distributions (clusters) about the $I_i = I_{i+1}$ line (Fig. 4E). However, for any given multiple of the period, the distribution of interspike intervals was not as large as that observed in periodically driven sensory neurons of the integrate-and-fire model with a random walk to threshold. The latter is readily appreciated by comparing the width of individual point clusters of the HH model (Fig. 4E) and cortical neuron (Fig. 1) return maps. Furthermore, the interspike interval density histograms (Fig. 4F) are not characterized by an exponential decay with higher multiples of the driving period as is typical of the primary sensory cortical neurons,[18] the random walk, integrate-and-fire model (Fig. 2C), or the periodically-driven noisy FitzHugh–Nagumo equations.[20] However, the transient nature and rare incidence of aperiodic activity for the HH equations under these conditions precludes a quantitative comparison.

3. DISCUSSION

The integrate-and-fire model has been explored as a plausible model of the periodically driven sensory cortical neuron. It is capable of simulating spontaneous activity. The sinusoidally forced integrate-and-fire model generates a restricted distribution of interspike intervals that cluster about one or more integer multiples of the stimulus period. When a random walk is introduced, this range is extended to include new interspike intervals at integer multiples of the stimulus period. Introduction of the random walk also leads the clusters of interspike interval pairs in the return map to be more diffuse and the width of individual peaks in the density histogram to increase, reflecting deviations around multiples of the driving period. Return maps of the sinusoidally driven integrate-and-fire model have little

asymmetry about the line $I_i = I_{i+1}$ or asymmetry within point clusters about rational multiples of the driving period. If a more complex, chaotic, function is used to drive the integrate-and-fire model, marked asymmetries appear along the line $I_i = I_{i+1}$ and within individual point clusters of the corresponding return map. Thus, some of the salient features observed in periodically driven sensory cortical neurons are reproduced with the sinusoidally driven integrate-and-fire model. However, the subtle asymmetries in distributions of the data are not realized without using a more complex (in this case chaotic) driving force. Thus, the integrate-and-fire model appears to emulate aspects of the neural data only when the synaptic input has nonlinear characteristics.

By design, the integrate-and-fire model described above has a nonlinearity in its input. It is also possible that the putative nonlinearities seen in the neural data are a result of intrinsic nonlinearities of the neuron. To test this possibility, the HH equations were stimulated with a sinusoidal input. Under these conditions, the HH differential equations reproduce some of the features observed in the interspike interval return maps from periodically driven sensory cortical neurons. Like the sinusoidally driven integrate-and-fire model with a random walk, the HH equations yield an extended range of interspike intervals all of which are close integer multiples of the driving period. In addition, sinusoidally driven HH equations can yield asymmetries in the density and clustering of interspike interval pairs about the line $I_i = I_{i+1}$. These complex interspike interval distributions and corresponding return maps are only generated within a restricted region of the frequency–amplitude parameter space for the sinusoidally driven HH equations. This restricted region is characterized by unstable phase locking to the driving period. Thus, although the intrinsic nonlinearities of the HH equations can give rise to some of the properties of the neural data, they seem to be lacking as a complete model.

There are other factors *in vivo* which may account for the properties of the data which are not modeled by the HH equations. The effects of noise on the HH frequency–amplitude parameter space have not been explored. Adding pseudorandom membrane fluctuations to the HH equations might provide a better model of the complex temporal patterns seen *in situ* as is known in squid axon.[6] In addition, shifting the HH equations into a oscillating state prior to coincident periodic driving broadens the regions of quasiperiodic activity.[8] Presumably, these manipulations broaden the regions of quasiperiodic activity yielding return maps with extended interspike interval distributions and asymmetries akin to those observed *in situ*. Thus, there are two possible mechanisms that may underlie the fingerprint structure of interspike interval return maps observed *in situ*. However, it is difficult to identify the physiological correlates for

such noise or oscillations. We are investigating a third possibility, that the extended range and prominent asymmetries of the interspike interval return maps are a consequence of interactions within a deterministic populations of neurons—without the imposition of an external noise source or intrinsic oscillatory properties.[18] We can mimic many of these properties of *in situ* data with a simple network of interconnected HH equations. Further elucidation of the fine structure awaits the study of the actual ionic processes and the functional (and synaptic) architecture of sensory cortical neurons *in situ* and perhaps the discovery of some general principles which underlie the temporal dynamics of neurons *in vivo*.

One might ask whether the fingerprint distribution of interspike interval return maps is pertinent to understanding sensory cortical information processing. Clearly, the local regions of asymmetry are not the same from neuron to neuron, whereas other features, such as the extended interspike interval range, are somewhat conserved for the same parameters. We suggest that these fingerprint distributions are reflecting some stable property or state of the network of neurons participating in the flash (or sensory) evoked activity of cortical neurons. In support of this hypothesis, the asymmetries are conserved with repetitive presentations of the periodic flash stimulus. Furthermore, preliminary cortical data suggest that the details of the interspike interval return maps change with stimulus parameters (e.g., bar orientation in primary visual cortex of cat; Siegel, unpublished results). Similarly, changes in temporal patterns of interspike intervals have been found when varying visual stimuli (Walsh basis sets) using quite different analytical approaches in inferior temporal cortex[13] as well as other subcortical and cortical regions. These studies suggest that neurons *do* encode sensory qualia in the temporal patterns of neurons. However, it remains an open and critical question whether the nervous system can actually use and exploit these temporal patterns to sense and explore the surrounding environment.

REFERENCES

1. S. H. Chung, S. A. Raymond, and J. Y. Lettvin, Multiple meaning in single visual units, *Brain Behav. Evol.* **3**:72–101 (1970).
2. M. J. Feigenbaum, Universal behavior in nonlinear systems, *Los Alamos Sci.* **1**:4–27 (1980).
3. G. L. Gerstein and M. Mandelbrot, Random walk models for the spike activity of a single neuron, *Biophys. J.* **4**:41–68 (1964).
4. G. L. Gerstein and D. H. Perkel, Mutual temporal relationships among neuronal spike trains. Statistical techniques of display and analysis, *Biophys. J.* **12**:453–473 (1972).
5. L. Glass, C. Graves, G. A. Petrillo, and M. C. Mackey, Unstable dynamics of a periodically driven oscillator in the presence of noise, *J. Theor. Biol.* **86**:455–475 (1980).

6. R. Guttman, L. Feldman, and E. Jakobsson, Frequency entrainment of squid axon membrane, *J. Membrane Biol.* **56**:9–18 (1980).
7. A. L. Hodgkin and A. L. Huxley, A quantitative description of the membrane current and its application to conduction and excitation, *J. Physiol.* (London) **117**:500–544 (1952).
8. A. V. Holden, The response of excitable membranes to a cyclic input, *Cybernetics* **21**:1–7 (1976).
9. A. Lasota and M. C. Mackey, *Probabilistic Properties of Deterministic Systems* (Cambridge University Press, Cambridge, 1985).
10. M. C. Mackey and A. Lasota, Noise and statistical periodicity, *Physica D* **28**:143–154 (1987).
11. V. B. Mountcastle, W. H. Talbot, H. Sakata, and J. Hyvarinen, Cortical neuronal mechanisms in flutter vibration studies in unanesthesized monkey neuron, *J. Neurophys.* **32**:45–84 (1967).
12. I. Nemoto, S. Miyazaki, M. Saito, and T. Utsunomiya, Behavior of solutions of the Hodgkin–Huxley equations and its relation to properties of mechanoreceptors, *Biophys. J.* **15**:469–479 (1975).
13. L. M. Optican and B. J. Richmond, Temporal encoding of two-dimensional patterns by single units in primate inferior temporal cortex, *J. Neurophysiol.* **57**:162–178 (1987).
14. H. Preissl, A. Aertsen, and G. Palm, Are fractal dimensions relevant for the description of neuronal activity? in *Parallel Processing in Neural Systems and Computers*, R. Bosch, ed. (1990), pp. 19–21.
15. P. E. Rapp, I. D. Zimmerman, A. M. Albano, G. C. Deguzman, and N. N. Greenbaum, Dynamics of spontaneous neural activity in the simian motor cortex: The dimension of chaotic neurons, *Phys. Lett. A* **110**:335–338 (1985).
16. R. W. Rodieck, N. Y.-S. Kiang, and G. Gerstein, Some quantitative methods for the study of spontaneous activity of single neurons, *Biophys. J.* **2**:351 (1962).
17. R. Shaw, *The Dripping Faucet as a Model Chaotic System* (Aerial Press, Santa Cruz, California, 1984).
18. R. M. Siegel, Non-linear dynamical system theory and primary visual cortical processing, *Physica D* **42**:385–395 (1990).
19. F. Takens, Detecting strange attractors in turbulence, in *Geometry Symposium: Utrecht 1980*, D. Rand and L.-S. Young, eds. (Springer, Berlin, 1981).
20. A. Longtin, *J. Stat. Phys.* **70**:309–327 (1993).